DYNAMIC ANALYSIS AND TESTING OF A SINGLE GIMBAL CONTROL MOMENTUM GYROSCOPE

Nicolae Tanase[1,2], Cristinel Ilie[1], Dragos Ovezea[1], Ionel Chirita[1], Marius Popa[1,2], Romulus M. Mihai[1,3], Mihai Guțu[1]
[1] National Institute for Research and Development in Electrical Engineering ICPE-CA, Splaiul Unirii no. 313, 030138, District 3, Bucharest
[2] Polytechnic University of Bucharest - UPB – Doctoral School of Electrical Engineering Splaiul Independenței nr. 313, Sector 6, Bucharest, Romania
[3] Valahia University from Târgoviște, Dâmbovița County, 130004, Romania
E-mails: nicolae.tanase@icpe-ca.ro, cristinel.ilie@icpe-ca.ro , dragos.ovezea@icpe-ca.ro, ionel.chirita@icpe-ca.ro, marius.popa@icpe-ca.ro, romulus.mihai@icpe-ca.ro, mihai.gutu@icpe-ca.ro

Abstract – Control Momentum Gyroscope (CMG), are the most complex moment control devices, capable of producing on the spacecraft torques obtained by combining two movements: one similar to that performed in the case of Momentum Wheels MW (a rotation of an inertial mass around an axis) with one axis of rotation perpendicular to the axis of inertial mass, this second axis being called the gyroscopic axis. The paper presents design of a Single Gimbal Control Moment Gyroscope (SGCMG) and mathematical model of dynamic analysis for a Single SGCMG. Based on the mathematical model it has been performed simulations of SGCMG using SolidWorks Simulation Premium (Motion Analysis). The results from the simulations are compared with tests performed on a testing stand for SGCMG developed at ICPE-CA.

Keywords: Control momentum gyroscope, Mathematical model, Dynamic analysis, Testing.

1. Introduction

A spacecraft is a vehicle designed to operate, with or without a human crew, in a controlled orbit or trajectory, located outside the lower atmosphere of the Earth, so at altitudes above 65 km [1-5].

Most spacecrafts do not have their own propulsion systems, in general they depend on a launch system that separates from the spacecraft after ensuring that it is positioned in a certain orbit around the Earth or imprints a certain initial speed on it which allows to detach from the Earth's gravitational field and launch on a path away from Earth.

Main types of spacecrafts [1-5]: *satellites* are spacecraft intended for observing the Earth or other cosmic objects or phenomens (stars, planets, comets, asteroids, etc.), of telecommunications, military, navigation, weather, recognition, etc .; *space probes* are unmanned spacecrafts designed to explore outer space, so they are printed at a speed of detachment from the Earth's gravitational field and placed on a path away from Earth; *experimental capsules* are spacecrafts which include a small laboratory with equipment for collecting various data and which are usually recovered after the mission; *modules and space shuttles* are manned spacecrafts with auxiliary launch system (space modules) or own (space shuttles), intended for various missions of limited duration; *space stations* are large spacecrafts placed on Earth orbit and equipped to support human crews for long periods of time.

Although spacecrafts differ greatly in design and structure, there are nine main categories of subsystems found in most spacecraft, namely: Power supply; Own propulsion; Communication system; ***Position control system***; Spacecraft temperature control system; Navigation system; Data calculation and processing system; Spacecraft structure, supporting all other subsystems; Spacecraft status and load monitoring system. From these, in this paper, the systems for controlling the position of spacecrafts have been approached.

Attitude Control Systems (ACS) have the role of stabilizing spacecrafts and directing them in the desired direction, during their mission and against the disruptive moments to which these vehicles are subjected [1-5].

The most important characteristics of a spacecraft are the mass (which must be as small as possible in order to have the lowest possible energy

consumption for transport to the destination and operation) and the reliability (which must be as high as possible, both due to high costs of the vehicle it self, but also of the transported equipment, as well as the practically impossibility of repairs, especially in the case of unmanned vehicles. It should also be remembered that during the mission, spacecrafts are exposed to extreme factors such as space vacuum, microgravity, impact with micrometeorites or debris from other space missions, extreme temperature variations and intense radiation.

The description of the position of a spacecraft must be made linked to a coordinate system defined in relation to the body of the spacecraft, such as that in Fig. 1. Because spacecraft is more of a rotational motion than a translational one, the position of the vehicle is described and can be controlled by means of three angles of rotation around the three main axes passing through the center mass of the vehicle, called [1-5]:

- rolling (longitudinal axis X);
- pitch (transverse axis Y);
- yaw (vertical axis Z).

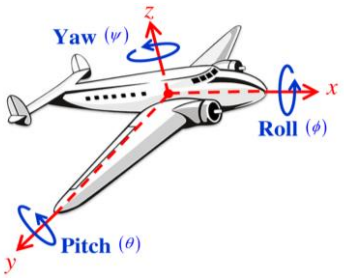

Figure 1: Coordinate system axes of a spacecraft [4].

Of course, a cubic-shaped satellite has no wings, tail, or nozzle, like the aircraft in Fig. 1. In such cases a coordinate system consisting of the main axes of the spacecraft body, those passing through the center mass of the vehicle and the angles of roll, pitch and yaw in relation to these axes shall be adopted.

There are three types of spacecraft position control actuators that operate on the basis of momentum conservation [6-10]:

- Reaction Wheel - RW;
- Momentum Wheel - MW;
- Control Momentum Gyroscope - CMG.

Reaction Wheels - RW, are primary spacecraft position control systems, usually used only during the repositioning of the vehicle (for example, for repositioning a telescope in a new direction). In the nominal state the speed of an RW is zero, for the rotation of the spacecraft in a certain direction it is necessary to rotate the RW in the opposite direction and only until the vehicle reaches the desired position.

Momentum Wheels – MW, are similar to RW from a constructive point of view, the difference between them being that, unlike RW which, as mentioned, have zero nominal speed, MW has zero non-nominal speed. In this way, by creating an angular momentum with a fixed orientation, the spacecraft is given increased stability in the direction of the MW axis of rotation, and when it is necessary to rotate the spacecraft, the total momentum value of the spacecraft is changed by changing only the speed value angle of the MW, not its direction. Position control systems equipped with MW usually use only one such device, no more than two.

Control Momentum Gyroscope – CMG, are the most complex control devices of the moment, capable of producing on the spacecraft torques obtained by combining two movements : one similar to the one made in the case of Momentum Wheel - MW (a rotation of an inertial mass around a axis) with one of the axis of rotation tillting, but about an axis perpendicular to the axis of inertial mass, this second axis being called the gyroscopic axis.

The output torque produced by the combination of the two mentioned movements has the direction perpendicular both to the direction of rotation of the inertial mass of MW and to the direction of the gyroscopic axis, as can be seen in Fig. 2.

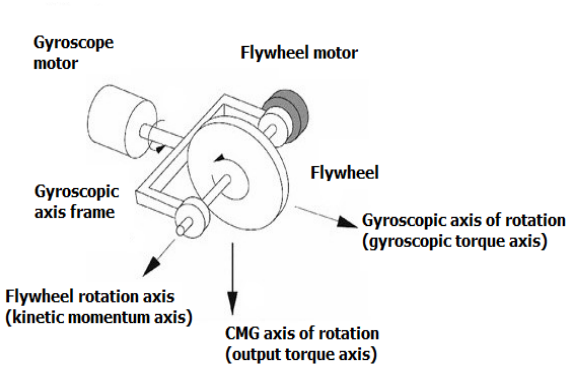

Figure 2: Schematic diagram of a CMG [2].

Single Gimbal Control Momentum Gyroscope SGCMG are CMGs with a single gyroscopic axis, in which the resulting torque is always perpendicular to both the angular momentum direction and the gyroscopic torque direction; due to the axis of the angular momentum intends to describe a precession motion under the action of the gyroscopic torque. Maintaining the resulting torque axis in a fixed direction is difficult, as CMG control requires a much more complicated algorithm than in the case of RW.

The gyroscopic moment control system shown in Fig. 2 is a mechanism that produces torque through a combination of two movements - rotating a flywheel around an axis called the flywheel axis and rotating the flywheel on an axis perpendicular to the flywheel axis called the gyroscope axis. The two main components of a CMG system are the flywheel and the gyroscope [7-10].

2. The Mathematical Model for the Dynamic Analysis of CMG

An object driven in rotational motion is subject to Newton's laws of motion, acquiring an agular momentum whose value depends on the shape of the object, mass distribution and the size of the angular velocity applied to the object.

In order to establish the motion equations of a CMG it will be used the principle scheme from Fig. 3 [9].

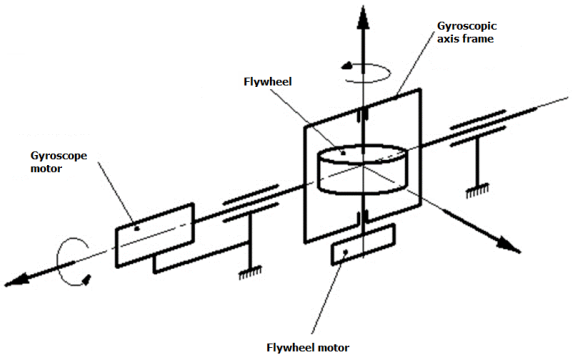

Figure 3: Computational scheme of a CMG.

The total angular momentum of the CMG is given by:

$$\vec{H}_{CMG} = \vec{H}_F + \vec{H}_G = I_F \cdot \vec{\omega}_F + I_G \cdot \dot{\delta}_G , \qquad (1)$$

where, $\vec{T}_{CMG}$ - the total torque acting on the CMG; $\vec{H}_{CMG}$ - the total angular momentum of the CMG in relation to the center mass of the spacecraft;
$\vec{H}_F$ - angular momentum of inertial mass (Flywheel - F), in relation to the center mass of the spacecraft;
$\vec{H}_G$ - angular momentum of the gyroscopic axis (Gimbal - G), in relation to the center mass of the spacecraft;
I_F - moment of inertia of the inertial mass;
I_G - moment of inertia of the gyroscopic axis;
$\vec{\omega}_F$ - angular velocity of the inertial mass;
δ_G - the tilt angle of the gyroscopic axis;
$\dot{\vec{\delta}}_G$ - angular velocity of the gyroscopic axis;

According to Euler's law, the total torque acting on the CMG is given by the rate variation of the angular momentum $\vec{H}_{CMG}$, so it will have the expression:

$$\vec{T}_{CMG} = \frac{d}{dt}(\vec{H}_{CMG}) =$$
$$= \frac{d}{dt}(I_F \cdot \vec{\omega}_F) + \frac{d}{dt}\left(I_G \cdot \dot{\vec{\delta}}_G\right) + \dot{\vec{\delta}}_G \times (I_F \cdot \vec{\omega}_F) = \qquad (2)$$
$$= I_F \cdot \dot{\vec{\omega}}_F + I_G \cdot \ddot{\vec{\delta}}_G + \dot{\vec{\delta}}_G \times (I_F \cdot \vec{\omega}_F)$$

In (2) it is observed that occurs $\dot{\vec{\omega}}_F$ - the angular acceleration of the inertial mass and $\ddot{\vec{\delta}}_G$ - the acceleration of the gyroscopic axis. The torques due to these accelerations are not used for CMG control and they occur only at the beginning and end of the rotational movements of the inertial mass and the gyroscopic axis. Basically, during the control of the spacecraft, both the inertial mass and the gyroscopic axis rotate at constant angular velocities, so the two accelerations are zero:

$$\dot{\vec{\omega}}_F = 0; \quad \ddot{\vec{\delta}}_G = 0 \qquad (3)$$

Thus the final expression of the gyroscopic torque acting on the CMG and implicitly on the spacecraft is given by the relation:

$$\vec{T}_{CMG} = \dot{\vec{\delta}}_G \times (I_F \cdot \vec{\omega}_F) , \qquad (4)$$

Depending only on the moment of mass inertia of the I_F inertial mass and the angular velocities $\vec{\omega}_F$ and $\dot{\vec{\delta}}_G$, of the inertial mass and the gyroscopic axis, respectively. It should be noted that (4) is valid in the hypothesis given by (3), neglecting the torques due to the accelerations from starting and stopping the inertial mass and the gyroscopic axis. This applies to large spacecrafts, in which the torque given by (4) has much higher values compared to the torques given by the angular accelerations of the inertial mass and the gyroscopic axis, $\vec{\omega}_F$ and $\dot{\vec{\delta}}_G$.

For small spacecraft, however, the torques due to these two accelerations are considerable in relation to the gyroscopic torque given by (4) and cannot be neglected. In addition to the torques due to the accelerations $\dot{\vec{\omega}}_F$ and $\ddot{\vec{\delta}}_G$, there are also the frictional torques that occur in the bearings of the inertial mass, the gyroscopic axis and the slip ring used to transmit power and control signals to the inertial motor. All of these torques are considered uncontrolled disturbing torques, and they can significantly affect the positioning of a picosatellite using a CMG device or greatly complicate the control of the CMG device.

3. Dynamic Simulation of CMG

In order to perform the numerical modeling using SolidWorks 2021 software, a 3D CAD model of CMG was made, this model being presented in Fig. 4. In order to reduce the computational time for simulation, a simplified model was designed. The finite element module of Motion Analysis was used from SolidWorks 2021 for the numerical simulation [11]. The friction in the bearings as well as the external disturbances that occur in CMG operation

were not taken into account for the simulation, the whole assembly without support weighing ~ 60 g.

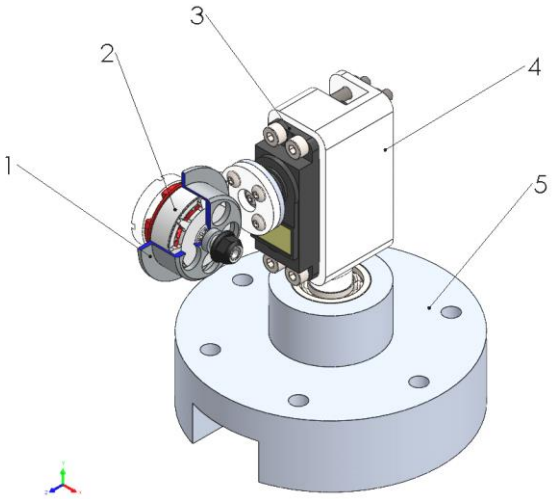

Figure 4: Single Gimbal Control Momentum Gyroscope CMG - 3D CAD model.

The system consists of a flywheel (1) made of stainless-steel DIN EN 1.4401 (X5CrNiMo17-12-2) which has a moment of inertia $I = 4.2\ kg * mm^2$, a BLDC motor type 2550KV (2) from EMAX which is rotating around the *Ox* axis at speeds from 2,500...18,000 RPM as well as a servomotor (gyroscopic axis) (3) SER0038 from DFROBOT, which can tilt around the *Oz* axis with values from $0...\pm 90^0$, both being controlled PWM (1-20 ms). The system also includes a servomotor support (4) as well as a support for mounting on a stand (5) for the entire assembly that allows a single degree of freedom - DOF (rotation of the entire CMG assembly relative to the *Oy* axis to determine the resulting angular momentum).

Based on the mathematical model presented above, the dynamic simulation of the CMG system was performed using the Motion Analysis module from SolidWorks 2021. In Fig. 5 is shown the diagram of the angular momentum variation in a prescribed time of 5 s for a speed of 13,000 RPM of the BLDC motor-flywheel and values of the tilt angle of the gyroscopic axis, between $0...+ 90^0$.

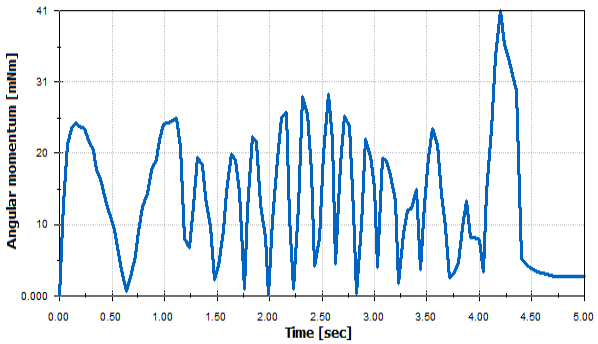

Figure 5: Variation of the angular momentum of the CMG system - dynamic simulation 13,000 RPM.

From Fig. 5 results a maximum value was obtained from the dynamic simulation of the angular momentum of T_{CMG} = 41.095 mNm at a maximum girosocpic axis tilt angle of $+ 90^0$.

Fig. 6 shows the variation of the angular momentum in time for a maximum speed of 18,000 RPM and $+ 90^0$ tilt angle of the gyrosocpic axis.

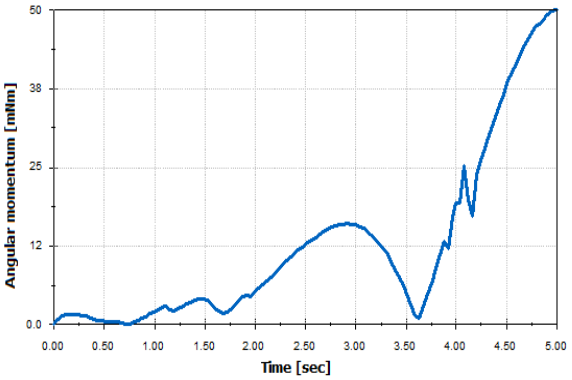

Figure 6: Variation of the angular momentum of the CMG system - dynamic simulation 18,000 RPM.

As can be seen in Fig. 6, at a speed of 18,000 RPM of the flywheel-motor at a maximum tilt angle of $+ 90^0$, an angular momentum was obtained resulting from T_{CMG} = 52.49 mNm using the configuration of the flywheel mentioned above.

4. The Test Stand of the CMG

The stand designed and made, whose principle scheme of electronic assembly is given in Fig. 6, is used to determine the characteristics of CMG with the possibility of measuring various parameters such as speed, spatial orientation, rotation of the gyroscopic axis, the moment generated.

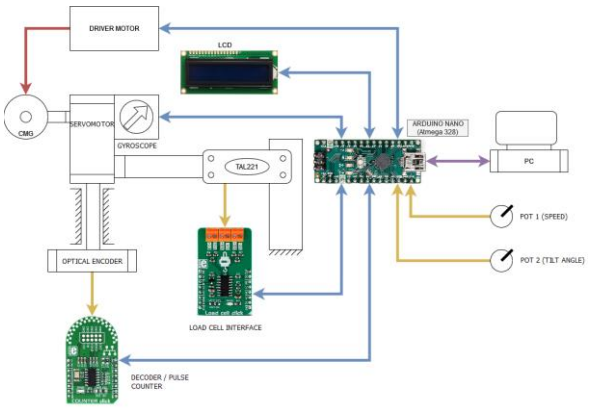

Figure 7: Block diagram of the stand for CMG testing.

An Atmega328 series microcontroller was used to control the electronic devices on the stand. It was selected because it is implemented on the Arduino UNO Rev.3 platform in the Atmega328P-U format that can be extracted from the socket and mounted

in a dedicated electronic circuit. The Arduino NANO platform [12] is also available, which uses the same microcontroller but in a more compact capsule can be mounted on a board type "bread-board".

The electronics in the block diagram (Fig. 7) were physically mounted on a test board (Fig. 8) whose primary use will be to perform the stand program, check the operation of the modules, command and control for CMG testing.

On the test board were mounted:

• a module with Atmega328 microcontroller, type Arduino NANO (1);

• a signal processing module (Load Cell Click) for tensometric marking force measurement systems based on the HX711 circuit (3);

• a (Counter Click) decoder / counter module for optical incremental encoders based on the LS7366R integrated circuit (4);

• a 9-axis accelerometer module based on the MPU9250 circuit (5);

• a level adapter for I2C that allows communication with 3.3V powered circuits (Atmega328 has an I2C interface with a logic level of 5V) (6);

• a buffer SN74LS07N integrated circuit with hollow collector outputs to allow the PWM signal level to be adjusted from 5V to 3.3V (7);

• a semi-adjustable potentiometer (8) by adjusting a voltage between 0 and 5V, which, read by the microcontroller, is used as a reference value for setting the control that regulates the motor speed;

• an adapter interface for displays with the HD44780 controller to the I2C protocol using PCF8574 [8], an eight-bit I / O expander;

• a 2x16-character alphanumeric display based on the Hitachi HD44780 control module (10).

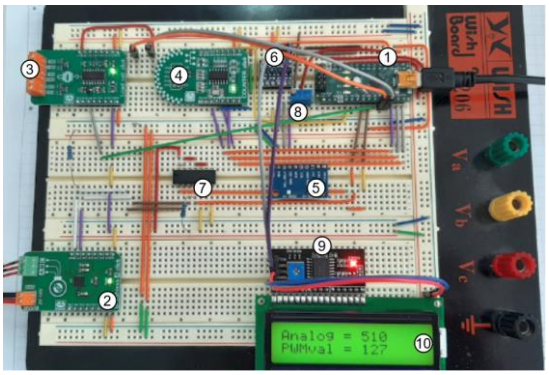

Figure 8: Electronic circuit of the test stand.

In (Fig. 9 a) and b)) you can see the overall image of the stand entirety, consisting of the following components: the experimental model of the CMG system (1), Manson SSP-8160 power supply (2), test and control board for CMG system (3), tachometer type AX-2901 (4), oscilloscope type GDS-2202E [13] (5), load cell 500 g, type SEN-FOR-28 [14] (6) in Fig. 9 a) and alternatively dynamometer with spring of 3 N (6 ') in Fig. 9 b).

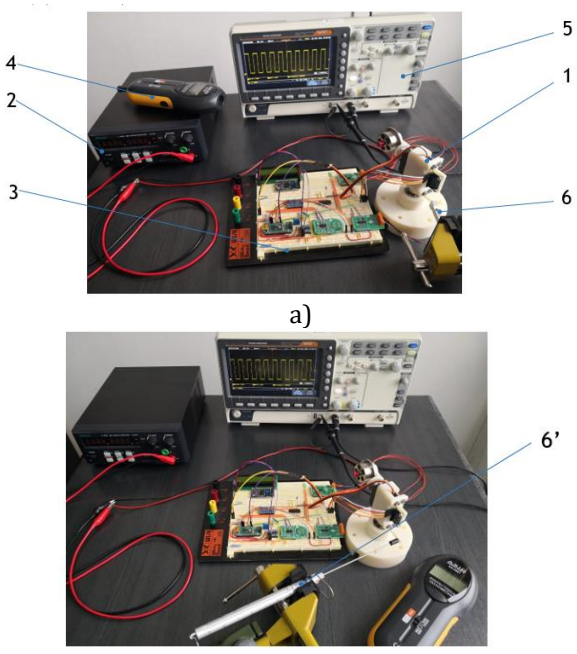

Figure 9: Stand for testing the CMG system.

5. Testing Program of the CMG

Regaring the test of the CMG system, a program has been made that automatically tests and records the data. The test program was written in C ++, in the Arduino IDE 1.8.13 (Fig. 10).

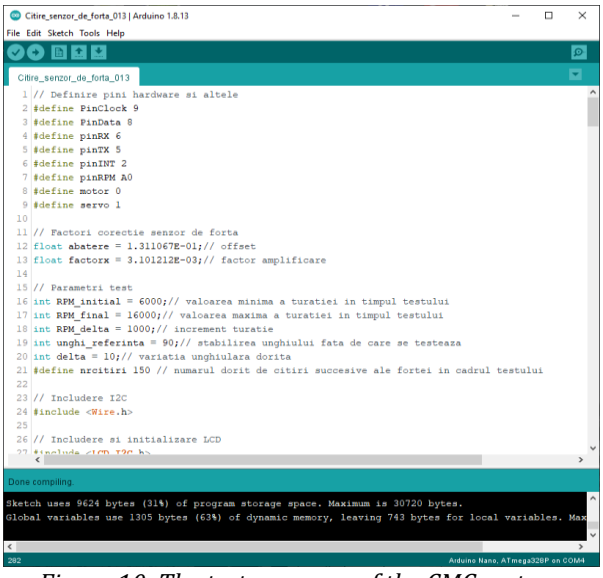

Figure 10: The test program of the CMG system.

As can be seen, the required pins are defined, after which the correction factors for the force sensor are recorded. Following the definition of the test parameters specifying the initial and final speed and the increment of its value, but also the reference angle from which the servomotor starts and the angular increment with which it moves.

This includes the libraries for the I2C protocol, the library for the LCD display with the I2C interface,

and the library for the PWM generation module. These are initialized.

A series of variables needed to run the program are then defined.

A "CLS_scaling" class is defined, that contains some functions necessary for the conversion of angle or speed values into PWM pulses of known duration, according to the calibration measurements made for the servomotor and the CMG motor. This class is instantiated outside of the setup () and loop () functions so that it can be available inside both.

In the setup () function, the pins previously defined as inputs or outputs are initialized, the first data on their status are read, is initialized the LCD display, the I2C port, the virtual COM port, the serial communication with the Maestro PWM. It also defines the parameters that make the connection between the angular position of the actuator and the duration of the PWM pulses that control the position.

The CMG system is brought to its original state by writing a 90° angle and 1,000μs pulses to the servomotor to indicate "zero speed" and to avoid entering the programming mode when the power is turned on.

Virtual COM and LCD warning messages are sent to the user announcing that he has 10 seconds to turn on the power supply and initialize the ESC 30A controller. After this time, "START test!" is displayed, and the main program starts running.

The loop () function contains two major instructions, a FOR loop and the STOP () function. The FOR loop sets a speed in the specified range and at that speed calls run_test (). After the FOR loop is completed, the program is stopped using the STOP () function which resets the servomotor and CGM motor to the initial conditions (90° angle and 0 RPM speed) after which it waits in infinite loop to disconnect the power supply and the PC connection cable to be able to copy and process data recorded on the serial monitor.

To change the test parameters, they are modified in the source code and the new program is recompiled and loaded on the microcontroller, an operation described by the manufacturer that takes less than a minute.

After running the experimental phase of the test, the data is copied from the serial port monitoring program and saved in <*.CSV> format. This file is opened and processed by a program written in LabVIEW [15]. It reads the data, corrects the deviation from zero, transforms the force value obtained into moment by multiplying the size of the lever fixed on the force sesor from the test stand and allows the resulting data to be exported to an Excel file.

The interface of this program can be seen in Fig. 11 and the code in Fig. 12.

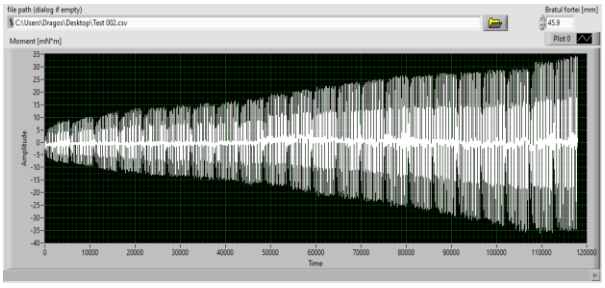

Figure 11: Data processing program interface.

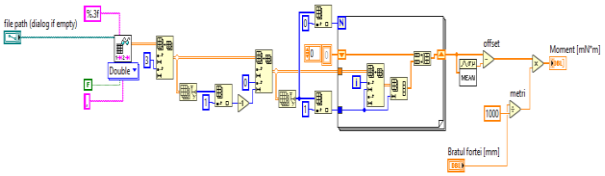

Figure 12: Data processing program code.

6. Experimental Testing of CMG

To perform the tests of the CMG system based on the program described above and according to a testing procedure developed by ICPE-CA, a series of tests of the whole assembly were performed. The command/control program described above allows running for testing and data generation automatically, for flywheel - motor speed between 2,500...16,000 RPM which performs measurements with the tilt angle of the gyroscopic axis between 0... $\pm 90^0$. In Fig. 13 is presented the testing stand of the CGM system in the final version, during the tests performed.

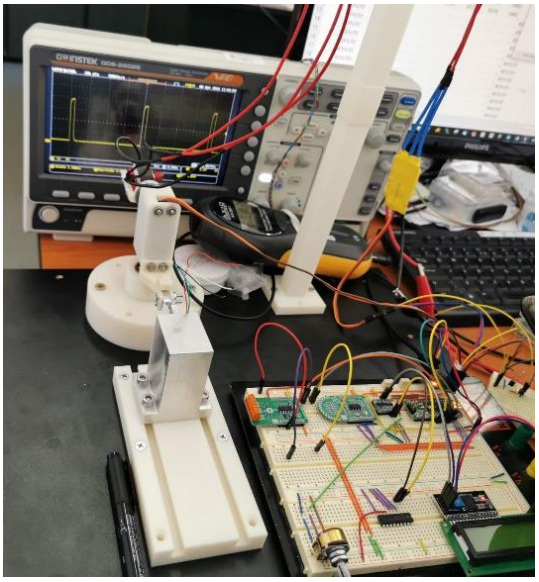

Figure 13: Experimental testing of CMG on stand.

The tests were performed with a flywheel made of stainless steel DIN EN 1.4401 (X5CrNiMo17-12-2) which has a moment of inertia I = 4.2 kg*mm^2, at speeds between 2,500 ... 13,000 RPM with a step of 500 RPM.

The force measurements were performed to determine the resulting angular momentum, with tilting the gyroscopic axis at angles between 0...± 90^0 with a step of 5^0. The diagram of measurement results are shown in Fig. 14.

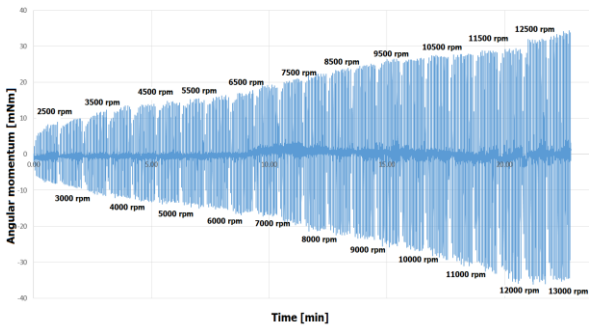

*Figure 14: Variation of the angular momentum of the CMG system for a flywheel with I = 4.2 kg*mm².*

As can be seen from Fig. 14, at a speed of 13,000 RPM of the flywheel-motor at a tilt angle of 90^0, a resulting angular momentum of T_{CMG} = 36.134 mNm was obtained using the flywheel configuration mentioned before.

Also using the above mentioned flywheel configuration, namely a stainless steel flywheel with a moment of inertia I = 4.2 kg*mm², two sets of angular displacement measurements of the CMG system were performed for speeds between 2,500-3,000 RPM by tilting the gyroscopic axis at angles between 0...+90^0 with a step of 10^0, the results of the angular displacement of the CMG system being presented in Fig. 15.

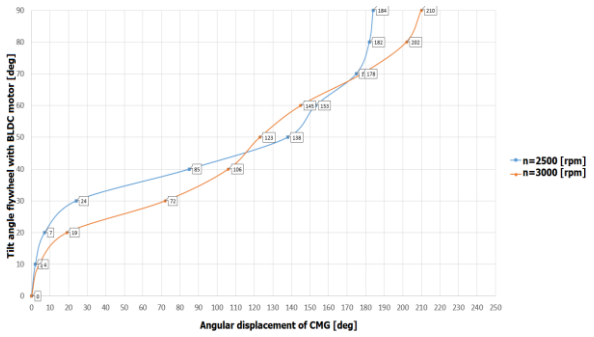

Figure 15: Angular displacement of the CMG system

As can be seen in Fig. 15, at a speed of 3,000 RPM of the flywheel-motor at a maximum tilt angle of 90^0, a stable angular displacement (without oscillations) of 210^0 for the CMG system was obtained, which represents a precise positioning of a space system.

Based on the previous results, a new set of tests of the CMG system (force measurements for determining the resulting angular momentum) was performed using another flywheel made from the same material (stainless steel), which has a higher moment of inertia, I = 10.9 kg*mm², at speeds between 6,000...12,000 RPM with a step of 1,000 RPM, tilting the gyroscopic axis at angles between 0...±90^0 with a step of 10^0. The results of the measurements are shown in Fig. 16.

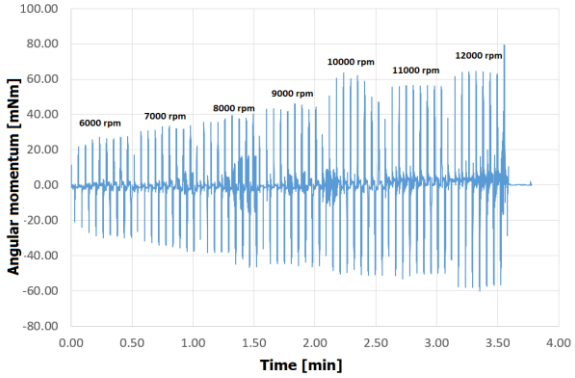

*Figure 16: Variation of the angular momentum of the CMG system for a flywheel with I = 10.9 kg*mm²*

As can be seen from Fig. 16, the CMG system was limited to a speed of 12,000 RPM, because the configuration designed made with the available materials did not allowed us to increase the speed of the flywheel motor to the maximum prescribed value of 16,000 RPM/18,000 RPM. Thus, using the configuration of the mentioned flywheel at a tilt angle of gyrosocpic axis of +80^0, a resulting angular momentum of T_{CMG} = +78.06 mNm was obtained, which can allow the orientation of voluminous spacecraft systems, having the dimensions arround tens of millimeters.

7. Conclusions

The paper presents a mathematical model of dynamic analysis for a CMG system, as well as simulations performed with the Motion Analysis module using the capabilities of SolidWorks 2021 software, which shows that with the change of flywheel speed and the tilt angle of the CMG increases the resulting angular momentum. Thus, for a flywheel speed of n = 13,000 RPM and a tilt angle of the gyroscopic axis of +90^0 an angular momentum of T_{CMG} = 41.095 mNm was obtained, respectively at a speed of n = 18,000 RPM and the same maximum tilt angle of the gyroscopic axis of +90^0, T_{CMG} = 52.49 mNm was obtained.

The test stand presented in this paper has a specific electronic assembly, created for testing the CMG system whose components allow the generation of PWM signal for motor speed control; generation of PWM signal for controlling the angle of the CMG tilting servomotor (gyroscopic axis); recording the signal values received from a load cell sensor with potentiometric marks, for measuring the developed torque; display relevant data from an alphanumeric LCD screen.

The CMG system was tested on the test stand according to a testing procedure developed by ICPE-CA and a maximum angular momentum

characteristic of the system designed T_{CMG} = 36.134 mNm was measured at a speed of 13,000 RPM of the flywheel-motor at a tilt angle of the gyroscopic axis of 90^0, with a flywheel which has a moment of inertia I = 4.2 kg*mm^2 which is comparable to the results obtained from the dynamic simulation, namely T_{CMG} = 41.095 mNm, which can be explained by the fact that in the numerical simulation the frictions of the system were not taken into account. At the same time, tests were performed with another flywheel, and an angular momentum was obtained resulting T_{CMG} = +78.06 mNm at a speed of 12,000 RPM, at a tilt angle of the gyrosocopic axis of $+80^0$, for a flywheel that has a moment of inertia I = 10.9 kg*mm^2. The angular displacement measurements were also performed and a 210^0 angular displacement of the CMG system was obtained at a speed of 3,000 RPM of the motor-flywheel that has a moment of inertia I = 4.2 kg*mm^2, at a maximum tilt angle of 90^0.

Finally, the possibilities to improve the design of the CMG subassemblies and the overall system performance were identified, namely: reducing the overall dimensions and weight of the CMG system to obtain the same performances; reducing system vibrations that occur during low speeds operation; the use of different materials and shapes of the flywheel to achieve a higher angular momentum.

Acknowledgements

The authors acknowledge the support offered through the PN19310304-46N/2019 research grant, also this work was supported by the Romanian Ministry of Education, Research and Digitalization, project number 25PFE/30.12.2021 – Increasing R-D-I capacity for electrical engineering-specific materials and equipment with reference to electromobility and "green" technologies within PNCDI III, Programme 1.

References

[1] ***https://www.britannica.com/science/spaceflight#ref741338, accesed on: 12.06.2019.

[2] S.A.V. Schallig, Q.P. Chu, S.W. Rhee, E. Van Kampen, Maximum Null Motion Algorithm for Single Gimbal Control Moment Gyroscopes, Advances in Aerospace Guidance, Navigation and Control, Springer International Publishing AG, Pp: 689-707, 2018. https://doi.org/10.1007/978-3-319-65283-2_37.

[3] *** Research grant PN19310304/2019 raport, ICPE-CA, Bucharest.

[4] H. A. Hashim, Special Orthogonal Group SO(3), Euler Angles, Angle-axis, Rodriguez Vector and Unit-Quaternion: Overview, Mapping and Challenges, arXiv preprint, 2019. arXiv:1909.06669.

[5] F.L. Markley and J.L. Crassidis, Fundamentals of Spacecraft Attitude Determinationand Control, Space Technology, Library 33, Springer Science+Business Media, New York, 2014. DOI:10.1007/978-1-4939-0802-8__1

[6] Bedrossian, N.S., Paradiso, J., Bergmann, E.V., and Rowell, D. Redundant single gimbal control moment gyroscope singularity analysis, Journal of Guidance, Control, and Dynamics, vol. 13, nr. 6, Pp. 1096-1101, Published Online:23 May 2012. https://doi.org/10.2514/3.20584

[7] R. O. Doruk, Nonlinear controller designs for a reaction wheel actuated observatory satellite, PhD Thesis, Middle East Technical University, Turkey, 2008.

[8] Vivek Nagabhushan, Development of Control Moment Gyroscopes for Attitude Control of Small Satellites, Master Thesis, University of Florida, 2009.

[9] Niklas Baker, Feasibility and design of miniaturized Control Moment Gyroscope for a 3-axis stabilized Micro Satellite, Space Engineering, masters level, Luleå University of Technology, 2016.

[10] Sinan Basaran, Selim Sivrioglu, and Erkan Zergeroglu, Composite Adaptive Control of Single Gimbal Control Moment Gyroscope Supported by Active Magnetic Bearings, Journal of Aerospace Engineering, Volume: 30, Issue Number: 1, 2016, ISSN: 0893-1321. DOI: 10.1061/(ASCE)AS.1943-5525.0000673

[11] *** SolidWorks, Motion Analysis 2021.

[12] *** https://www.arduino.cc/ accesed on: 11.04.2022.

[13] *** https://www.gwinstek.com/en-global, accesed on: 15.04.2022.

[14] *** http://www.htc-sensor.com/, accesed on: 06.12.2021.

[15] *** LabVIEW 2020.